



Sensitivity of seasonal flood simulations to regional climate model spatial resolution

Mariana Castaneda-Gonzalez¹ · Annie Poulin¹ · Rabindranath Romero-Lopez² · Richard Arsenault¹ · François Brissette¹ · Richard Turcotte³

Received: 14 May 2018 / Accepted: 23 April 2019 / Published online: 3 May 2019
© Springer-Verlag GmbH Germany, part of Springer Nature 2019

Abstract

The potential impacts of floods are of significant concern to our modern society raising the need to identify and quantify all the uncertainties that can impact their simulations. Climate simulations at finer spatial resolutions are expected to bring more confidence in these hydrological simulations. However, the impact of the increasing spatial resolutions of climate simulations on floods simulations has to be evaluated. To address this issue, this paper assesses the sensitivity of summer–fall flood simulations to the Canadian Regional Climate Model (CRCM) grid resolution. Three climate simulations issued from the fifth version of the CRCM (CRCM5) driven by the ERA-Interim reanalysis at 0.44°, 0.22° and 0.11° resolutions are analysed at a daily time step for the 1981–2010 period. Raw CRCM5 precipitation and temperature outputs are used as inputs in the simple lumped conceptual hydrological model MOHYSE to simulate streamflows over 50 Quebec (Canada) basins. Summer–fall flooding is analysed by estimating four flood indicators: the 2-year, 5-year, 10-year and 20-year return periods from the CRCM5-driven streamflows. The results show systematic impacts of spatial resolution on CRCM5 outputs and seasonal flood simulations. Floods simulated with coarser climate datasets present smaller peak discharges than those simulated with the finer climate outputs. Smaller catchments show larger sensitivity to spatial resolution as more detail can be obtained from the finer grids. Overall, this work contributes to understanding the sensitivity of streamflow modelling to the climate model’s resolution, highlighting yet another uncertainty source to consider in hydrological climate change impact studies.

Keywords CRCM5 · Floods · MOHYSE · Return periods · Spatial resolution

1 Introduction

Extreme hydrological events such as floods constitute a recurrent problem that can cause pronounced social, economic, and environmental losses worldwide. Consequently, the number of studies evaluating the potential effects of

climate change on flooding has progressively increased (Dankers and Feyen 2008; Giuntoli et al. 2015; Kundzewicz et al. 2017; Veijalainen et al. 2010; Wehner et al. 2017). However, because there is only limited evidence and considerable uncertainty, confidence in projections of future changes in flood magnitude and frequency is still low (Kundzewicz et al. 2014, 2017). The literature identifies many sources of uncertainty in the hydroclimatic modelling processes used to evaluate climate change impacts on hydrology, and recognizes greenhouse emission scenarios, global climate model structures, downscaling methods, impact (or hydrological) models and natural climate variability as some of the most important sources of uncertainty (Falloon et al. 2014; Giuntoli et al. 2015; Kundzewicz et al. 2018; Wilby 2005).

Most studies generally considered the climate model to constitute the most significant source of uncertainty (Arnell and Lloyd-Hughes 2014; Hagemann et al. 2013; Wilby and Harris 2006). However, recent studies have analysed other

Electronic supplementary material The online version of this article (<https://doi.org/10.1007/s00382-019-04789-y>) contains supplementary material, which is available to authorized users.

✉ Mariana Castaneda-Gonzalez
mariana.castaneda-gonzalez.1@ens.etsmtl.ca

¹ École de technologie supérieure, 1100 Notre-Dame Street West, Montreal H3C 1K3, Canada

² Universidad Veracruzana, Lomas del Estadio S/N, Zona Universitaria, Xalapa 91000, Mexico

³ Ministère du Développement durable, Environnement et Lutte contre les changements climatiques, 675 boulevard René Lévesque Est, Québec, QC G1R 5V7, Canada

sources of uncertainty related to General Circulation Model (GCMs) and Regional Climate Model (RCMs) configurations. Roy et al. (2014) showed that the largest source of uncertainty in seasonal simulations of precipitation extremes came from the climate model selection, the domain size and the member selection, each source with seasonal uncertainty differences. Another example is the impact of spectral nudging, a technique developed to ensure that the RCM simulations remain close to the driving fields during the downscaling process (Biner et al. 2000; Miguez-Macho et al. 2004; Storch et al. 2000). Different studies have analysed the impacts of spectral nudging reaching contrasting conclusions (Mearns et al. 2018; Separovic et al. 2012). For example, Alexandru (2009) confirmed ‘side-effects’ such as the reduction of precipitation extremes, while other studies recommend its application to reproduce daily weather regimes, seasonal anomalies and large-scale conditions (Lucas-Picher et al. 2015a; Sanchez-Gomez et al. 2009). Thus, additional uncertainties and impacts can be expected when spectral nudging is applied to RCM simulations. It has been observed that other sources of uncertainty can also be present in the hydro-climatological modelling chain. Therefore, the research community is continuously looking to identify and quantify the types of uncertainty that are most important for each particular impact study (Beven 2016; Hawkins et al. 2013; Vetter et al. 2017).

During the last decade, GCMs have been downscaled with higher resolution RCMs. This has led to improvements in the representation of climate variables within the hydrological cycle, and suggested that using RCMs was more adequate for studies at local scales (Terai et al. 2017; Teutschbein and Seibert 2010; Wehner et al. 2014; Wehner et al. 2010). Many studies have examined how the increasing spatial resolution of RCMs impacts climate outputs (Chan et al. 2013; Mahajan et al. 2015; Terai et al. 2017; Wehner et al. 2010, 2014; Zeng et al. 2016) showing strong sensitivities to resolution changes. Overall, finer precipitation and temperature simulations were closer to observations. However, these improvements were mixed and inconsistent as mean statistics showed to be more realistic in coarser resolutions over some regions. Some studies have evaluated the effects of finer RCM grids on precipitation simulations, presenting evidence of the commonly named “added value” from the use of finer spatial resolutions to simulate extreme climate events (Curry et al. 2016b; Lucas-Picher et al. 2016). Recently, very high resolution RCM simulations (kilometer-scale) known as *convection-permitting* have been tested in different regions of the world (Kendon et al. 2017; Prein et al. 2015; Sandvik et al. 2018). The high-resolutions (e.g., 2–10 km) allow convective storms to be better represented, yet the added value is still inconsistent and variable depending on spatial heterogeneities (i.e., topography) and temporal scales (Ekström and Gilleland 2017; Prein et al. 2013, 2015).

Discrepancies have also been found in the effects of spatial resolution on other variables such as temperature. For example, studies have shown reductions in temperature biases when using finer spatial resolutions, but at the expense of a decrease in variability (Hertwig et al. 2015; Klavans et al. 2017). These results show that the refinement of spatial resolution brings additional uncertainties which must be taken into account in climate modelling.

As science and computing resources evolve, there is a clear trend towards a finer spatial resolution for both GCMs and RCMs. As observed in climate model outputs, it is also expected that finer resolutions will modify and improve the representation of the hydrological processes for studies at the basin scale. Regional studies at the basin scale typically use GCM or RCM climate projections as inputs to hydrological models to produce estimates of current and future streamflows and to analyse uncertainties associated with the simulation process. In North America, the Canadian Regional Climate Model version 5 (CRCM5) outputs have been used to simulate flood events (Lucas-Picher et al. 2015b; Teufel et al. 2017). These studies showed that CRCM5 using fine grids (0.09° and 0.11°) was able to reproduce spatio-temporal features of particular extreme events in Canada yet difficulties were observed to represent the peak discharges. Other studies have focused on modelling floods under future climate change projections and the quantification of the uncertainties involved (Alfieri et al. 2015; Arnell and Lloyd-Hughes 2014; Dankers et al. 2014; Das and Umamahesh 2018; Roudier et al. 2016; Wasko and Sharma 2017). However, the impact of varying horizontal resolution has been neglected by using the finest climate simulations available. Studies at local scales using climate simulations can be found in large numbers in different regions (Chen et al. 2011; Graham et al. 2007; Kundzewicz et al. 2014; Minville et al. 2008; Naz et al. 2016; Riboult and Brissette 2015; Trudel et al. 2017) compared to the much fewer studies focusing on the analysis of RCM spatial resolution effects on streamflow simulations, and particularly on hydrological extremes such as floods. Among the latter studies, Dankers et al. (2007) evaluated high resolution RCM simulations (12 km and 50 km) over a European river basin, showing a generally better representation of precipitation patterns and extreme events from finer simulations when compared to meteorological observations. However, no clear improvements or considerable differences were found in streamflow simulations at various gauging stations. On the other hand, at the sub-basin scale, better simulations of extreme hydrological events were observed when using high resolution RCM data. Shortly after, a climate change impact study on flood hazards over Europe performed by Dankers and Feyen (2008) confirmed the mixed impacts of spatial resolutions previously obtained in Dankers et al. (2007). At the regional scale, Graham et al. (2007) investigated how the use

of different RCM simulations affected hydrological changes in the Lule River Basin in northern Sweden. Although the paper focused on approaches for transferring the signal of climate change to hydrological models, considerable seasonal differences were observed when using finer resolutions (25 against 50 km resolutions). However, the benefits of using higher resolution regarding peak flows were still inconclusive. Focusing on the simulation of flood events, Lobliqueois et al. (2014) investigated the impacts of higher resolution rainfall data on streamflow simulations over a diversity of catchments (181 in all) in France, and yet found no systematic impact among them. It was concluded that the hydrological response was highly variable between catchments, depending on their size and the specific characteristics of each particular rainfall event. More recently, Mendoza et al. (2016) assessed the effects of RCM simulations at three different spatial resolutions (4 km, 12 km and 36 km), as well as their spatial aggregation on hydrological projections, over three catchments of the Colorado River Basin in the United States. Their results suggested that the RCM spatial resolution had significant effects on mean annual runoff projections, which were shown to be larger than the effects of the spatially aggregated climate data. Moreover, in line with Lobliqueois et al. (2014)'s results, improvements in streamflow simulation were observed in the largest catchments where the most heterogeneous precipitation patterns were found.

These previous studies provided a wide range of results concerning the impact of RCM spatial resolution on both climate outputs and streamflow simulations. Of particular note, these studies do not show any systematic impact of spatial resolution on streamflow simulation, and especially on flooding events. The differences between methodologies and selected evaluation approaches in the previous studies make it difficult to assess the effects of finer climate data on flood simulations. It is also important to mention that all previous studies compared the streamflow simulations against observations while attempting to pinpoint the potential added value of finer spatial resolution. The use of an observational database induces many challenges (e.g., measurement errors, necessity to bias-correct climate model outputs) and additional uncertainties to take into account (Kundzewicz et al. 2017).

To address these different issues, this paper aims mainly to analyse the sensitivity of flood simulations to changes in the spatial resolution of CRCM5 outputs. The focus of the paper is on extreme rainfall events, occurring in the summer–fall seasons, which are expected to be better represented in finer resolutions, and on the floods directly related to these extreme events. Streamflow simulations for 50 river basins located in the southern province of Quebec are generated with a hydrological model fed with climate model precipitation and temperature outputs at three different

spatial resolutions (0.44° , 0.22° and 0.11°). Then, four flood indicators based on 2, 5, 10, and 20-year return periods are computed. The impact of CRCM5 spatial resolution on precipitation and temperature outputs (entire Quebec province territory) on simulated streamflows and on the flood indicators is then investigated. In the following section, the study area and the data used are described. The methodology is described in Sect. 3. Section 4 presents the main results and analysis, and discussion and conclusions are presented in Sect. 5.

2 Study area and data

2.1 Study area

This study was carried out over 50 river basins in central and southern Quebec, Canada. All 50 river basins are located within the Quebec computational domain of the CRCM5. Figure 1 shows the study area and the mean annual precipitation of each river basin, which ranges from 800 to 1400 mm per year. The river basins were selected to have a diversity of sizes ranging from 512 to 18,983 km² covering a total area of 176,842 km². They are all subject to snow accumulation as the main factor leading to flooding during the winter–spring period along with rain-on-snow events and convective storms during the summer–fall season, annual minimum and maximum temperatures are -23.5 and $+21$ °C averaged on all watersheds.

2.2 Data

2.2.1 Observed data

For this study, observed and RCM datasets were used. Observed data consisted of meteorological and hydrometric datasets. The observed meteorological data included daily maximum temperature, minimum temperature and precipitation values provided by the *Direction de l'expertise hydrique* (DEH) unit of Québec's *Ministère du Développement Durable, de l'Environnement et de la Lutte contre les Changements Climatiques* (MDDELCC). The meteorological database was derived by interpolating (simple kriging) observations from 971 stations operated by the MDDELCC and from 21 stations operated by Rio Tinto, a private hydro-power and metal smelting company. The interpolated dataset created a grid of 0.1° (≈ 11 km) resolution covering the domain from 43° to 55° latitude and 60°W to 80°W longitude. The observed hydrometric data consisted of daily streamflow at the river basin outlets. The database was obtained from the *Banque de Données Hydriques* (BDH) of the DEH on a daily time step for the 50 hydrometric stations. This database covered the 1969–2010 period. For each

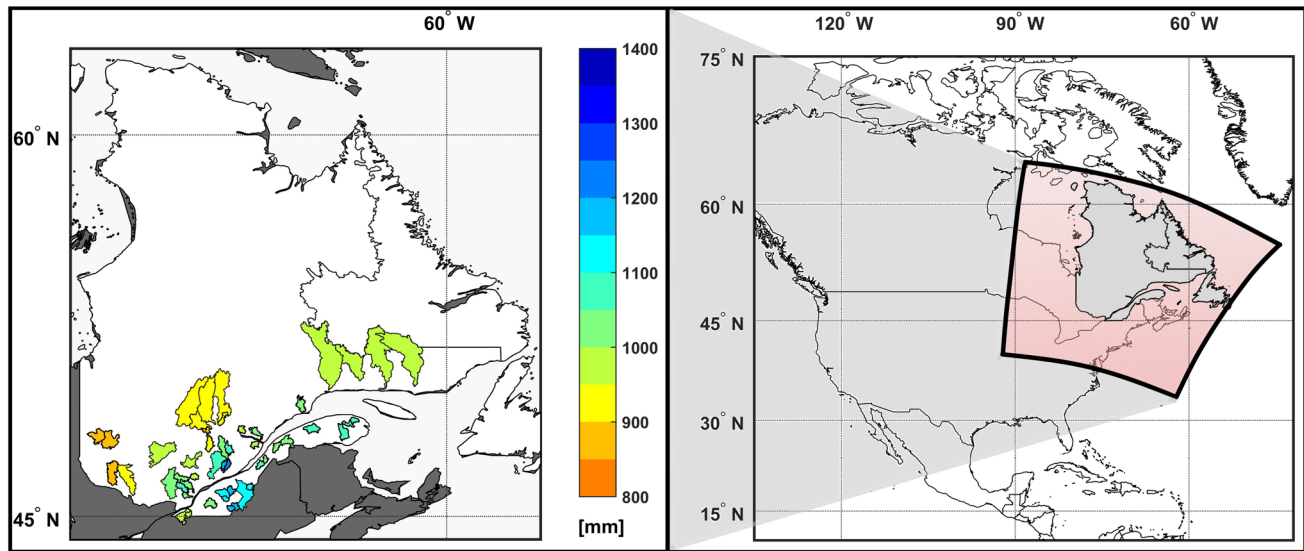


Fig. 1 Location and mean annual precipitation (mm) of the 50 river basins used in this study. The Quebec computational domain of the CRCM5 is presented in light red

basin, the common intersection between all hydroclimatic data was used. The minimum intersection length was at least 12 years.

2.2.2 RCM data

The RCM datasets consisted of minimum and maximum temperatures and precipitation available at a daily time step, and were all provided by the Ouranos Consortium on Regional Climatology and Adaptation. These climate datasets were issued from the CRCM5, developed at *the Centre pour l'Étude et la Simulation du Climat à l'Échelle Régionale* (ESCER) at the *Université du Québec à Montréal* (UQÀM) with the collaboration of Environment and Climate Change Canada (ECCC) (Côté et al. 1998; Irambona et al. 2016; Lucas-Picher et al. 2016; Martynov et al. 2013). The CRCM5 is based on a limited-area version of the Global Environment Multiscale (GEM) model used for Numerical Weather Prediction at ECCC (Côté et al. 1998; Martynov et al. 2013). Regarding the hydrological cycle, the CRCM5 physics package consists of deep and shallow convection schemes (Kain and Fritsch 1990; Kuo 1965; Teufel et al. 2017). A more detailed description can be found in Separovic et al. (2013) and in Martynov et al. (2013).

The three simulations used in this paper were performed at three different spatial resolutions, covering the 1981–2010 period, and using the same driver, namely, the ERA-Interim reanalysis, as well as the same domain (Quebec domain), as presented in Table 1. In other words, the only difference between the model simulations was the spatial resolution, which therefore allowed a targeted sensitivity analysis. Figure 2 shows the different elevation (m a.s.l.; upper panel

Table 1 Description of the CRCM5 climate datasets used in this study

| Acronym | Version | Driver | Domain | Resolution |
|---------|---------|----------------|--------|-------------|
| 0.11° | 5 v3331 | ERA-Interim 75 | Quebec | 0.11°≈12 km |
| 0.22° | 5 v3331 | ERA-Interim 75 | Quebec | 0.22°≈24 km |
| 0.44° | 5 v3331 | ERA-Interim 75 | Quebec | 0.44°≈48 km |

a) and the land area fraction (%; lower panel b) of the three simulations at different resolutions. All simulations were performed without spectral nudging over the Quebec domain.

3 Methodology

This study analyses the sensitivity of the summer and fall flood simulations to changes in the RCM spatial resolution. The methodology consists of three parts. The first part involves a comparison between climate simulations (temperature and precipitation) with different spatial resolutions to evaluate the impact on RCM outputs. The second part deals with the hydrological modelling processes needed to generate the RCM-driven streamflow simulations. Finally, the third part addresses the seasonal (summer–fall) flood simulation analysis using the 2-year, 5-year, 10-year and 20-year return periods as flood indicators. Figure 3 presents an overview of the methodology used for this study. As shown in Fig. 3, it is important to stress that observations are only used in this study to calibrate the hydrological model. Once calibration is complete, the rest of the work

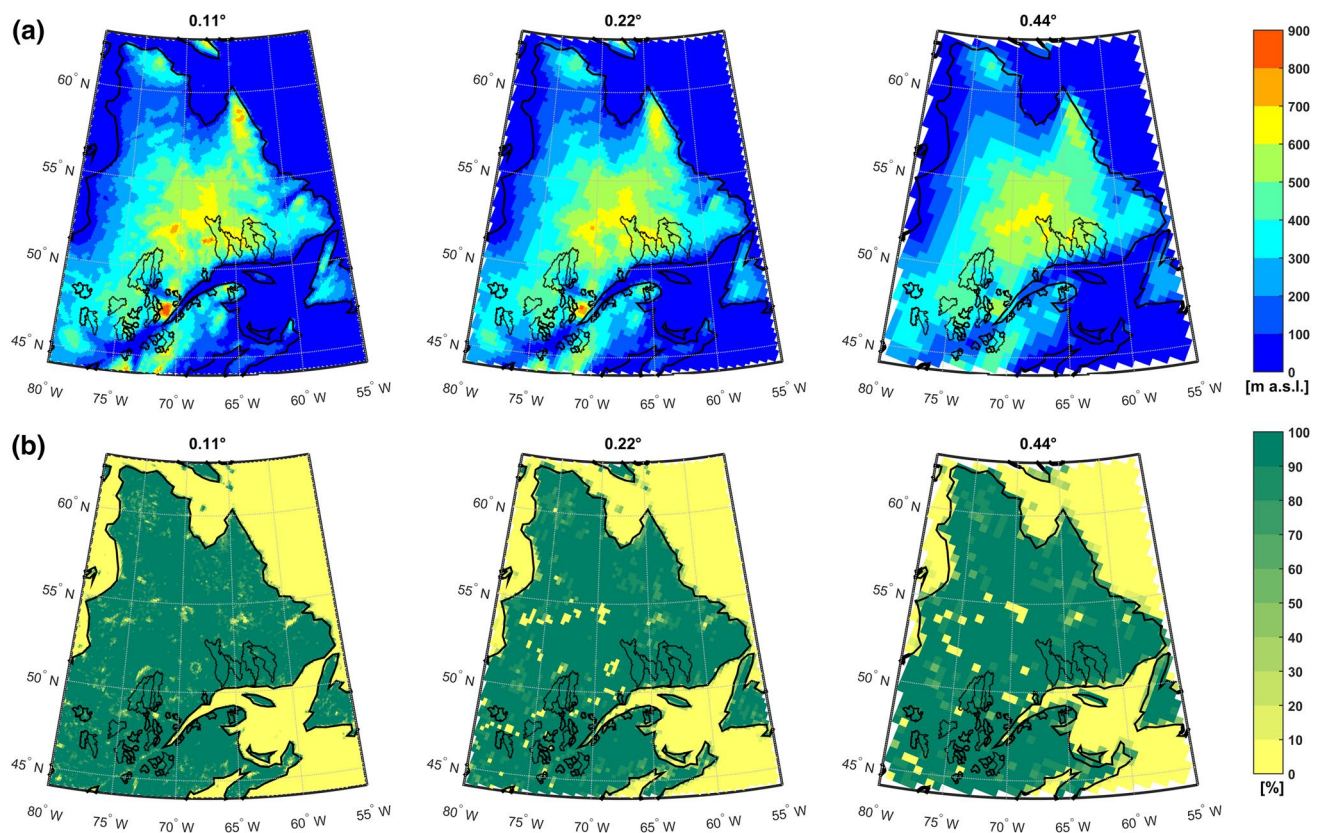


Fig. 2 Elevation (m a.s.l.) and land area fraction (%) of the three CRCM5 simulations with different resolutions. The upper panels **a** show the elevations at 0.11° , 0.22° and 0.44° resolutions. The lower panels **b** show the land area fraction at 0.11° , 0.22° and 0.44° resolutions

is performed using only model data in an intercomparison framework. Comparing against observations would demand some form of bias correction, which would largely remove differences between model outputs at different resolutions, and that would be detrimental to the main objective of this study. This will be further discussed later.

3.1 Climate simulations intercomparison

The first step of the methodology consists in evaluating the impacts of the RCM spatial resolutions (0.44° , 0.22° and 0.11°) on climate outputs (temperature and precipitation). The assessment is performed by comparing the differences between two climate simulations with different resolutions. Two comparisons are performed between the three climate datasets. The first intercomparison is performed between the 0.22° and the 0.11° resolution datasets (presented as $0.22^\circ/0.11^\circ$), where the 0.11° simulation is used as the reference dataset. The second intercomparison is performed between the 0.44° and the 0.11° resolution datasets (presented as $0.44^\circ/0.11^\circ$), also using the 0.11° simulation as the reference to directly compare the $0.22^\circ/0.11^\circ$ with the $0.44^\circ/0.11^\circ$. These two intercomparisons are performed for both temperature and precipitation. As observed in the

intercomparison configuration, the finer dataset (0.11°) is compared with the coarser datasets (0.22° and 0.44°). The purpose of this paper is to compare the coarser datasets to the finer dataset to quantify the potential ‘added value’ of the higher spatial resolution. For this reason the coarser (and older) datasets (0.22° and 0.44°) were compared against the finer (and latest) dataset (i.e., 0.11°). To that end, the 0.22° and 0.44° resolution datasets are downscaled at the resolution of the higher dataset (0.11°), creating a grid of the same size to allow the intercomparisons to be carried out between each grid point directly. The RCM datasets at different resolutions share the same geographical projection and grid structure, so the downscaling is simply performed by using the same value of the coarser dataset for each divided grid cell to match the finer dataset.

Performance statistics are computed to evaluate the differences between the climate simulations. Three metrics are used to evaluate the RCM outputs during the summer seasons (June, July and August) and fall seasons (September, October and November): the seasonal bias for temperature, the seasonal relative bias for precipitation, and the variance ratio for both temperature and precipitation simulations.

For the seasonal bias and seasonal relative bias, the comparisons are performed using the mean seasonal values for

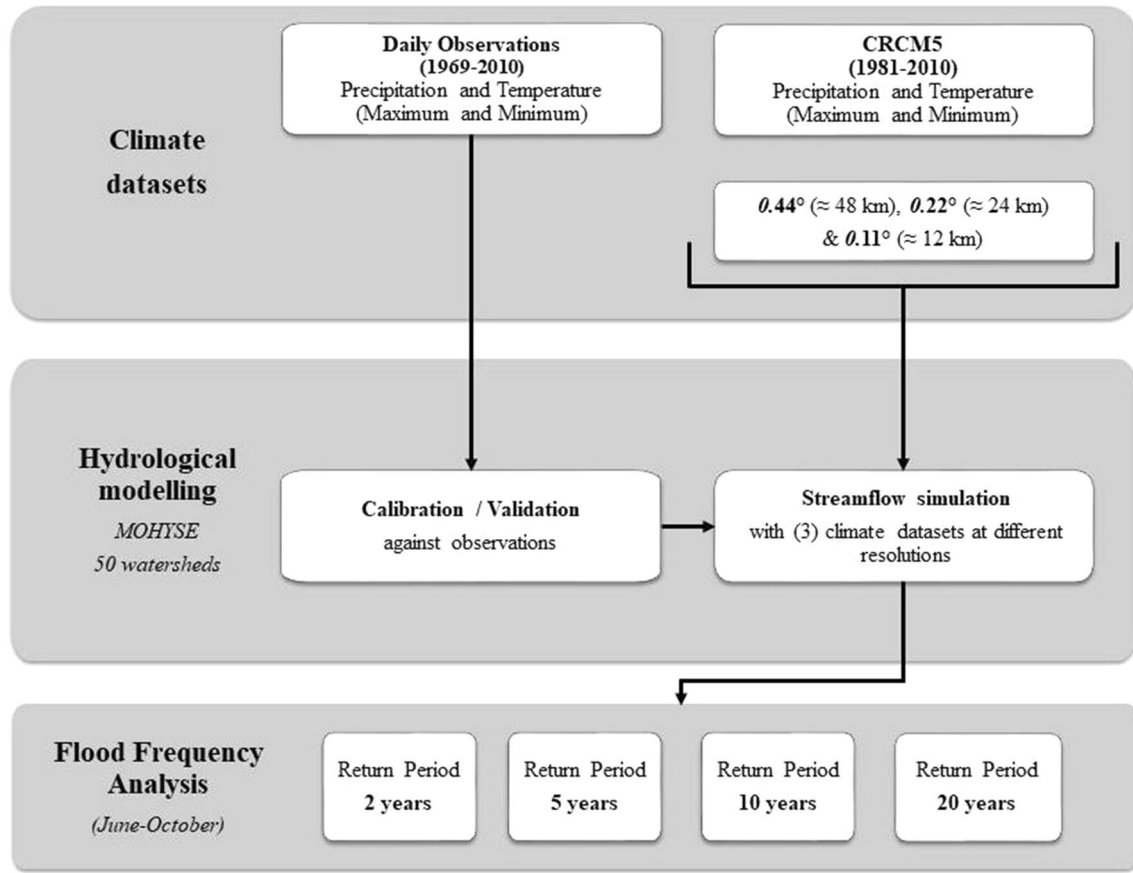


Fig. 3 Overview of this project's research methodology

temperature and precipitation datasets. The mean seasonal temperature (\bar{T}) and the mean seasonal precipitation (\bar{P}) are calculated as follows:

$$\bar{T} = \frac{\sum_{i=1}^{N_y} \sum_{j=1}^{N_s} T_{ij}}{N_y N_s} \quad (1)$$

$$\bar{P} = \frac{\sum_{i=1}^{N_y} \sum_{j=1}^{N_s} P_{ij}}{N_y N_s} \quad (2)$$

where T_{ij} and P_{ij} are the daily values of temperature and precipitation, N_s is the number of days of the season and N_y is the number of years of the full time series. The leap year day is removed from all the datasets.

The temperature seasonal bias is calculated between the mean seasonal temperatures of a given dataset x (i.e., 0.22° or 0.44° resolution dataset), named \bar{T}_x , and the mean seasonal temperatures of a reference dataset y (i.e., 0.11° resolution dataset), named \bar{T}_y , as follows:

$$B_T = \bar{T}_x - \bar{T}_y \quad (3)$$

The precipitation seasonal relative bias is calculated between the mean seasonal precipitations of a given dataset x (i.e., 0.22° or 0.44° resolution dataset), named \bar{P}_x , and the mean seasonal precipitations of the reference dataset y (i.e., 0.11° resolution dataset), named \bar{P}_y , as follows:

$$B_{P_{rel}}(\%) = \frac{\bar{P}_x - \bar{P}_y}{\bar{P}_y} \times 100\% \quad (4)$$

The ratio of the variances is the third metric used to evaluate the RCM outputs. This metric indicates whether the spatial resolution of the RCM impacts the variability of temperature and precipitation data, and the frequency of their seasonal extremes. The leap year day is also removed from the datasets. The seasonal variance (σ^2) ratio (temperature or precipitation) is then calculated between the mean variance of a given dataset x (i.e., 0.22° or 0.44° resolution dataset), named $\bar{\sigma}_x^2$, and the mean variance of a reference dataset y (i.e., 0.11° resolution dataset), named $\bar{\sigma}_y^2$, as follows:

$$\text{Ratio of the variances} = \frac{\bar{\sigma}_x^2}{\bar{\sigma}_y^2} \quad (5)$$

These metrics were selected to quantify the differences between the climate simulations with different spatial resolutions to evaluate their impacts and differences. Thus, it is important to recall that no comparison is made with actual observations.

3.2 Hydrological modelling

The hydrological modelling is performed by the simple lumped conceptual hydrological model, MOHYSE. This model has been largely used in research over the province of Quebec and was selected due to its availability, simplicity and relatively low computing resource requirements.

3.2.1 Description of the hydrological model

The MOHYSE model is a simple lumped conceptual model with ten parameters, which was first developed by Fortin and Turcotte (2006). The model has been used in different studies over Canadian watersheds, such as those by Velázquez et al. (2010), Arsenault et al. (2015) and Arsenault and Brissette (2016). MOHYSE simulates the main hydrological processes (e.g., potential evapotranspiration and snow melting and accumulation), and can be run on different time scales (from sub-daily to multiple days). The required inputs consist of mean daily temperatures and total daily precipitation (i.e., rain and snow), which are averaged over the basin area.

3.2.2 Calibration and validation

MOHYSE has ten parameters, which were automatically calibrated using the Covariance Matrix Adaptation Evolution Strategy (CMAES) (Hansen and Ostermeier 1997). This optimization algorithm was selected due to the good results presented by Arsenault et al. (2014) in the calibration of MOHYSE over different catchments. The hydrological model was calibrated in the odd years for the different available hydroclimatic periods for each watershed. This, as previously described in Sect. 2.2 consists of a minimum intersection length of 12 years between the 1969–2010 period. The hydroclimatic periods used for each watershed are included in the additional Online Resource 1. A validation was then performed in the even years for each of the 50 river basins. This approach has the disadvantage of requiring the calculation of streamflows for the entire time period during calibration, even though only the odd years are used to compute the objective function (OF). However, it has the great advantage of eliminating problems linked to natural climatic variability and anthropic climate change that are common when splitting the data record into two consecutive periods, one for calibration and one for validation (Arsenault et al. 2015; Essou et al. 2017). The calibration/validation was done using a customized

OF based on the modified Kling-Gupta Efficiency (KGE) (Gupta et al. 2009; Kling et al. 2012) as described in the following Eqs. (6)–(9):

$$KGE = 1 - ED \quad (6)$$

$$ED = \sqrt{(r - 1)^2 + (\beta - 1)^2 + (\gamma - 1)^2} \quad (7)$$

$$\beta = \frac{\mu_s}{\mu_o} \quad (8)$$

$$\gamma = \frac{CV_s}{CV_o} = \frac{\sigma_s/\mu_s}{\sigma_o/\mu_o} \quad (9)$$

where r represents the correlation coefficient between observed and simulated streamflows, β represents the bias ratio and γ represents the variability ratio. The ratio μ represents the mean streamflow, CV is the variation coefficient and σ represents the standard deviation of the streamflow. The “o” subscript represents the observed streamflow and the “s” subscript represents the simulated streamflow.

Possible KGE values range from—infinity to 1, where a value of 1 indicates a perfect fit between the datasets, a value of 0 means a good fit on average values, and a negative value indicates a worse fitting than using the mean as a predictor. The KGE criterion has been shown to overcome the problems related to the use of functions based on the mean squared error, such as strongly prioritizing runoff peaks and underestimating variability (Gupta et al. 2009), and as a result, its use has significantly increased in hydrological applications (Beck et al. 2016; Huang et al. 2016; Oyerinde et al. 2017; Thirel et al. 2015). Based on the qualitative evaluation criteria recently used in Crochemore et al. (2015) and Huang et al. (2016), median KGE values ≥ 0.7 are considered as “good” to “very good” performances.

As previously mentioned, the OF used in this study is a variation of the KGE criterion previously described in Eqs. (7)–(10). This customized criterion consists of two equal parts. The first is the KGE computed on the interannual mean hydrograph, and the second is the KGE computed on the daily time series of summer–fall months (June–October). This method was selected in order to specifically target the summer and fall flooding (the targeted seasons of the present study), while maintaining a realistic representation of the annual hydrograph. The OF used for calibrating the parameters can be expressed as follows:

$$OF = \frac{KGE_{interannual\ mean}}{2} + \frac{KGE_{summer-fall}}{2} \quad (10)$$

The optimal set of parameters was chosen based on the customized OF. The validation was then performed over the non-calibrated years of the same period. It is important to recall that the number of years used for the calibration/

validation varies between the 50 basins according to data availability as previously mentioned in Sect. 2.

3.2.3 Streamflow simulations

As described previously, the hydrological model MOHYSE was first calibrated and validated with historical observations of streamflows to evaluate its performance in the June–October floods. In this process, a set of model parameters was obtained for each of the 50 basins. Then, the CRCM5 climate datasets were used as inputs to the previously calibrated/validated hydrological model MOHYSE. In a typical study using climate model data for hydrological modelling, the outputs would be bias-corrected, or the hydrological model would be recalibrated to force a better match between computed and observed streamflows. In this study, great care was taken to ensure that any observed difference is only linked to the spatial resolution of the climate model. As such, a common parameter set must be used, and hydrological model recalibration or bias correction would automatically violate the above constraint, making the use of the parameter set used in the real world a reasonable alternative. Thus, it was assumed that the parameter sets derived from the hydrological model calibration/validation would be adequate to avoid possible impacts of hydrological models parameterization. It is important to state once again that this is an intercomparison study between CRCM5 outputs of different resolutions. No comparison will be made against observed datasets. Therefore, three climate-driven streamflow time series (one for each of the climate model resolutions) were generated and used in the intercomparison study.

The climate-driven streamflow simulation intercomparison was done following the same approach described for the climate datasets analyses. Two comparisons were performed between the three streamflow simulations: the first was the 0.22° resolution against the 0.11° resolution ($0.22^\circ/0.11^\circ$), and the second, the 0.44° resolution against the 0.11° resolution ($0.44^\circ/0.11^\circ$). To measure the difference between the evaluated datasets, these two comparisons were done by using the seasonal normalized root mean squared error (NRMSE), which is defined as follows:

$$NRMSE = \frac{\sqrt{\frac{1}{N_s} \sum_{i=1}^{N_s} (X_i - Y_i)^2}}{\bar{Y}} \quad (11)$$

where X_i is the daily simulated streamflow of the dataset X and Y_i is the daily simulated streamflow of the dataset Y used as a reference. \bar{Y} is the mean of the dataset Y and N_s is the number of days of the season of the full time series. The leap year day is again removed from the datasets. The NRMSE indicates the normalized difference between two datasets,

where a value of 0 indicates the perfect fit, and larger values indicate larger differences between the evaluated datasets.

3.3 Flood indicators

Four flood indicators were used to evaluate the effects of the RCM spatial resolution on the flood simulations: the 2-year, 5-year, 10-year and 20-year return periods of the summer–fall floods. As described in Sect. 2, the three CRCM5-simulated datasets used in this study have a length of 30 years. Thus, the four flood indicators were defined based on the dataset length (30 values of annual summer–fall peak flows) in order to have an appropriate sample size to estimate representative distributions for each return period. The four flood indicators were estimated by a flood frequency analysis using the Gumbel distribution for each simulated streamflow and each basin. The Gumbel distribution was selected for this analysis as it is frequently used in hydrology to represent flood peaks distributions due to its commonly good approximations and simplicity of use (Chebana and Ouarda 2011; Loaiciga and Leipnik 1999; Marques et al. 2015; Yue et al. 1999). The fitting of the Gumbel distribution was visually verified for each river basin (results not shown).

The flood values estimated for the four return periods were compared using the same approach previously described for the climate simulations and the streamflow simulations (see Sect. 3.1), namely, the $0.22^\circ/0.11^\circ$ and the $0.44^\circ/0.11^\circ$ analyses. The comparisons between the estimated return periods were done using the relative bias (%), which is defined as follows:

$$B_{rel}(\%) = \frac{X - Y}{Y} \times 100\% \quad (12)$$

where Y is the value used as the reference. This metric was selected to quantitatively evaluate the sensitivity of flood simulations to the RCM spatial resolutions for the four different return periods estimated from the generated climate-driven summer–fall peak flows.

4 Results

The results are presented in three main sections. First, comparisons between the climate simulations with different spatial resolutions are presented for the CRCM5-simulated temperature and precipitation. Next, the hydrological modelling performance is shown for calibration and validation years with respect to observed data over the 50 basins. Finally, the climate-driven streamflow simulations are compared and analysed by calculating the NRMSE over the streamflow simulations and the relative biases between the flood values for the four flood indicators (i.e., the 2-year, 5-year, 10-year

and 20-year return periods) estimated from the streamflow simulations at different spatial resolutions.

4.1 Climate simulations analysis

4.1.1 Temperature bias

Figure 4 presents the maps of the seasonal daily mean temperature ($^{\circ}\text{C}$) difference between simulations with different resolutions, the 0.22° resolution against the 0.11° resolution (upper panel a), and the 0.44° resolution against the 0.11° resolution (lower panel b). The figure shows the temperature difference for the summer seasons (JJA, on the left panels) and fall seasons (SON, on the right panels) over the province of Quebec. The 50 basins of the study area are highlighted in black. The results between the 0.22° and 0.11° resolutions (top two panels) show a consistent hot bias over the entire region during the fall months (SON). Smaller and generally hot biases are observed during the summer, with some cold biases observed close to the coastal areas and water bodies in the center of the province. Similar trends are also observed for the 0.44° and 0.11° resolutions comparison (bottom two panels), and yet the range of biases is slightly larger, reaching values of up to $3\ ^{\circ}\text{C}$ difference. It can also be seen that there are some pixels with suspiciously large biases at some otherwise unremarkable locations. These large differences

can be explained by the presence of large lakes and reservoirs that are resolved in the finer CRCM grid, but not in the coarser resolution ones. As observed in Fig. 2, the differences in the land area fraction masks used for the three simulations can create these large differences observed in the lake and reservoirs locations.

4.1.2 Precipitation relative bias

Figure 5 presents the relative biases between the CRCM5-simulated precipitations at different spatial resolutions. Both comparisons show similar seasonal trends. A general dry trend is observed during the summer months (JJA). On the other hand, during the fall months (SON), wet and dry relative biases are observed throughout the province. Overall, larger relative biases are observed between the 0.44° and the 0.11° resolution precipitation simulations (lower panel b).

4.1.3 Temperature and precipitation variance ratios

Figures 6 and 7 present the variance ratio maps of seasonal mean temperature and precipitation, respectively. Similar trends are observed between the two comparisons for both seasons. On the seasonal mean temperature variance ratio maps (see Fig. 6), the 0.22° and 0.44° resolution temperature simulations show a consistently smaller variance during

Fig. 4 Seasonal daily mean bias of temperature ($^{\circ}\text{C}$) between CRCM5 simulations with different resolutions for the summer (JJA) and fall (SON) seasons over the 1981–2010 time period. The upper panels a show the comparisons between datasets at 0.22° and 0.11° resolutions. The lower panels b show the comparisons between datasets at 0.44° and 0.11° resolutions

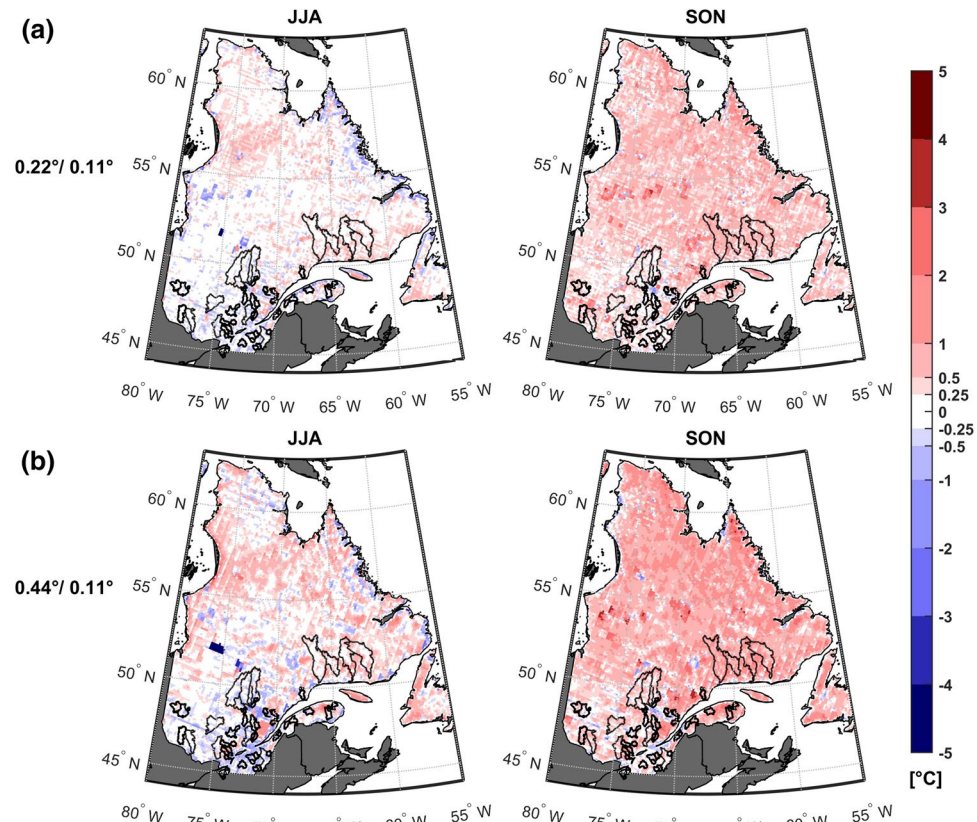


Fig. 5 Seasonal daily mean relative biases of precipitation (%) between CRCM5 simulations with different resolutions for the summer (JJA) and fall (SON) seasons over the 1981–2010 time period. The upper panels **a** show the comparisons between datasets at 0.22° and 0.11° resolutions. The lower panels **b** show the comparisons between datasets at 0.44° and 0.11° resolutions

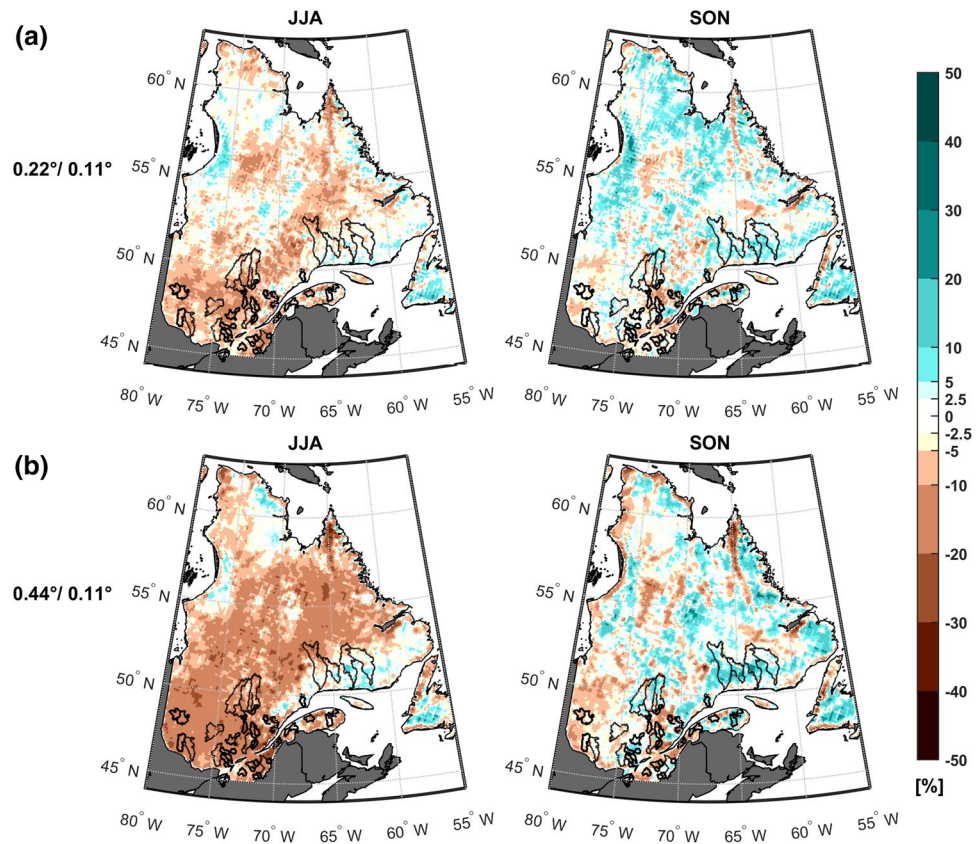


Fig. 6 Ratio of annual seasonal mean temperature variances between CRCM5 simulations with different resolutions for the summer (JJA) and fall (SON) seasons over the 1981–2010 time period. The upper panels **a** show the comparisons between datasets at 0.22° and 0.11° resolutions. The lower panels **b** show the comparisons between datasets at 0.44° and 0.11° resolutions

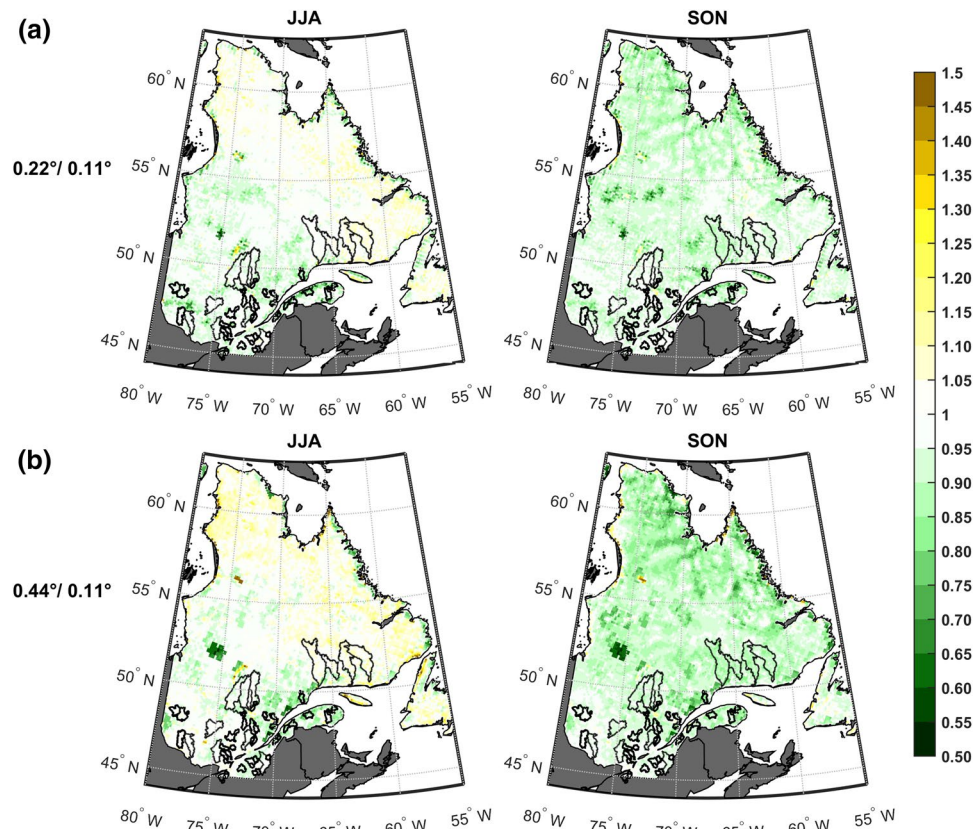
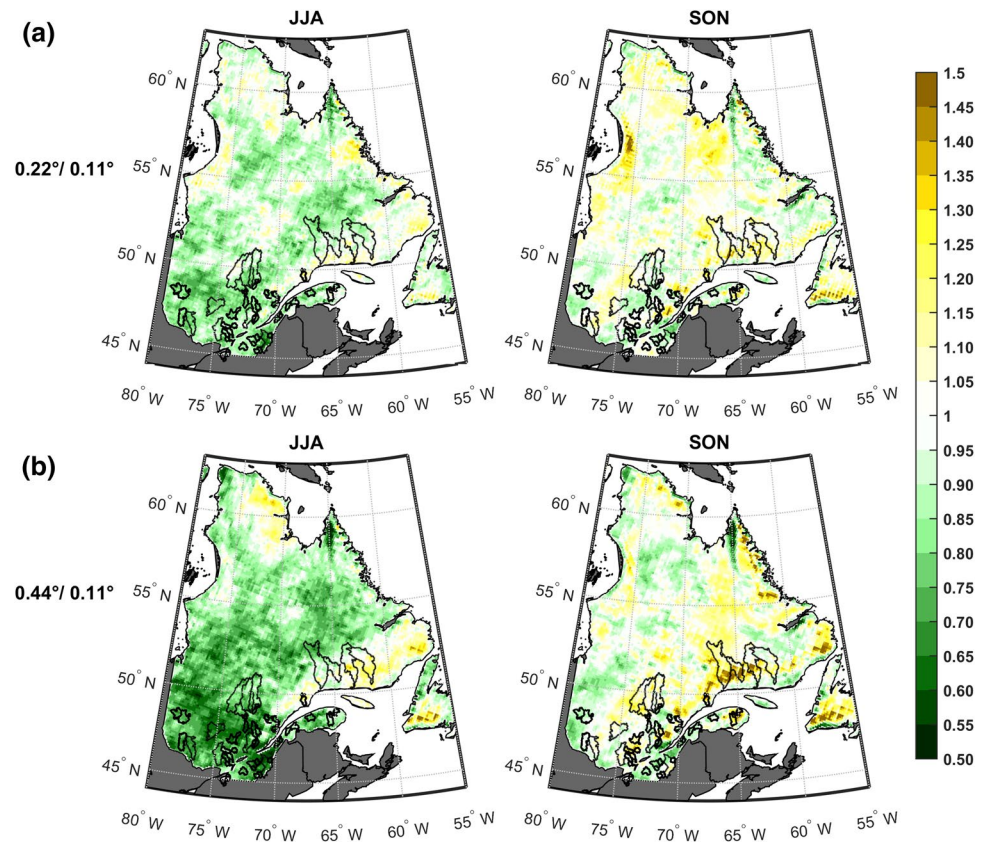


Fig. 7 Ratio of annual seasonal mean precipitation variances between CRCM5 simulations with different resolutions for the summer (JJA) and fall (SON) seasons over the 1981–2010 time period. The upper panels **a** show the comparisons between datasets at 0.22° and 0.11° resolutions. The lower panels **b** show the comparisons between datasets at 0.44° and 0.11° resolutions



the fall months in both comparisons. The variance differences reach values of up to 20–25% in the 0.44° and 0.11° resolutions comparison (lower panel b) and smaller variance differences (5–15%) in the 0.22° and 0.11° resolutions comparison. During summer months, a different trend is observed. The 0.22° and 0.44° resolution simulations show larger variances in the northeast, and smaller ones in the southwest, when compared to the 0.11° resolution simulation. Yet, slightly larger differences are observed between the 0.44° and the 0.11° resolution temperature data (see Fig. 6 lower panel b). Note the persistent outlier pixels corresponding to reservoirs and lakes which are not resolved similarly in all CRCM resolutions.

Seasonal similarities are observed in both comparisons in terms of the precipitation simulations variance ratio. During the summer season, the 0.22° and 0.44° resolution simulations show smaller variances in the south and center of the province when compared with the simulation at finer resolution. Yet, the variance differences increase when the 0.44° resolution simulation is considered (for up to 50%). During the fall months, smaller differences in variance are generally observed for both comparisons. Overall, differences in variance are slightly larger between the 0.44° and the 0.11° resolutions comparison (lower panel b) than between the 0.22° and the 0.11° resolution datasets (upper panel a) over the

province, and specifically in the studied basins, the observed differences are approximately 10 and 25%. Additional comparisons (0.44°/0.22°) are given in Online Resource 2.

4.2 Hydrological modelling

Figure 8 presents the calibration and validation performances of MOHYSE for the 50 basins. The KGE criterion was re-calculated over the complete simulated streamflows to evaluate the performance of the basins with the selected OF. The left panel a) displays the distributions (boxplots) of the KGE values measuring the basins performance over the full time series (blue boxplots) and the performance during the summer–fall months (red boxplots). Each boxplot is then constituted of 50 KGE values, one for each basin. On the right panel b), the KGE obtained in calibration is compared against the KGE obtained during validation for each basin. When the calibration produces better results than the validation, markers are displayed under the reference line, and when the validation outperforms the calibration, markers are displayed over the reference line.

Overall, according to the qualitative performance presented in Sect. 3, it is clear from Fig. 8 that MOHYSE performs well for both calibration and validation periods. Yet, differences are observed between the full time series and

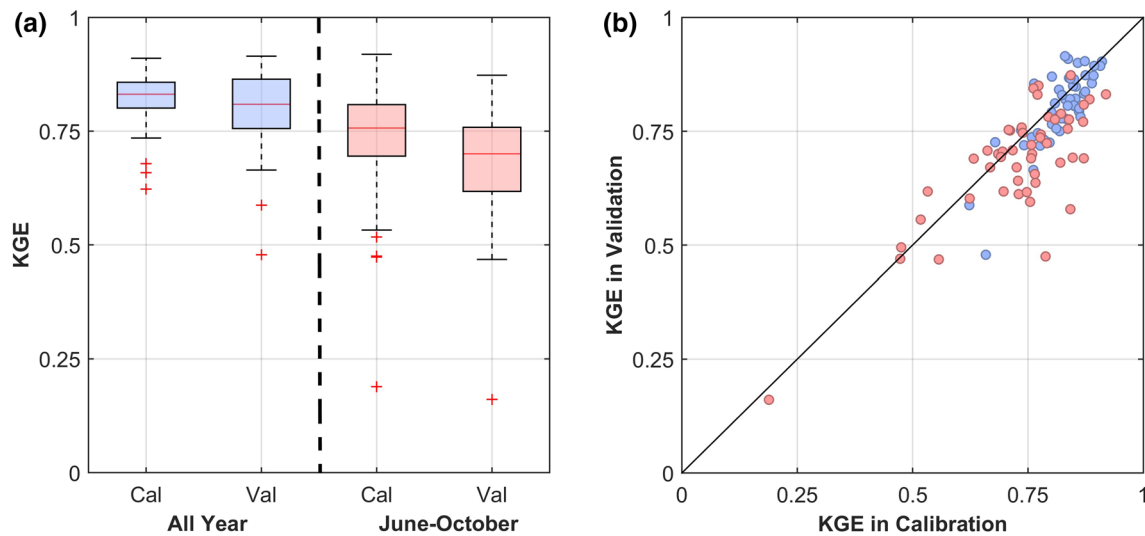


Fig. 8 KGE values for the calibration and validation years are presented for the full time series (blue) and the June–October months (red). Panel **a** presents the boxplots of the calibration and validation

the June–October evaluations. On the left panel a), the red boxplots show that MOHYSE has lower performance during the summer–fall months when compared with the full time series evaluations. However, it should be recalled that these catchments are snowmelt-dominated, and thus are naturally expected to have lower KGE values in rainfall-dominated periods (i.e., June–October). On the right panel b), in line with the results of the left panel a), MOHYSE clearly shows generally good and consistent performances during both the calibration and validation periods for each basin. The results in this panel also show the decreasing KGE values during the June–October streamflow simulations, as expected. The specific basins with bad performances also correspond to the outliers observed in the distributions of panel a). Overall, median KGE values of approximately 0.65 are observed during the summer–fall validation, while in the full time series results, they are over 0.75. Thus, following the Crochemore et al. (2015) and Huang et al. (2016) qualitative evaluation criteria based on full time series evaluations, MOHYSE presents a good performance.

4.3 RCM-driven streamflow simulations

Figure 9 shows the seasonal comparisons of streamflows simulated with CRCM5 outputs at different spatial resolutions, using the Normalized Root Mean Squared Error (NRMSE). The figure is divided into four sections. Each section shows one season, namely, winter (December, January and February), spring (March, April and May), summer (June, July and August) and fall (September, October and November) from left to right. For each season, the two

for both evaluations. On panel **b**, the KGE in calibration is compared against the KGE in validation for each basin

defined comparisons are presented, i.e., the $0.22^\circ/0.11^\circ$ and the $0.44^\circ/0.11^\circ$.

In Fig. 9, smaller differences are observed in the streamflow simulation comparison between the 0.22° and the 0.11° resolutions (dark green) than between the 0.44° and the 0.11° resolutions (light green). These results are observed consistently during the four seasons. During the summer months (June, July and August) the largest differences (higher median NRMSE values) and wider boxplots are clearly observed. Generally, during each of the four seasons, it is observed that the larger the difference in the RCM spatial resolution, the larger the difference between streamflows.

In Fig. 10, the relative biases between the flood values for the different return periods estimated from the simulated summer–fall peak streamflows are presented. The four flood indicators show a clear relative bias increase in the summer–fall flood return periods, along with a refinement in spatial resolution. In other words, the $0.22^\circ/0.11^\circ$ boxplots present smaller differences than the $0.44^\circ/0.11^\circ$ boxplots. This behaviour is observed in the distributions of the four flood indicators, where the comparisons between the 0.22° and the 0.11° resolution return periods (dark blue) show nearly no bias, with median values closer to zero. Moreover, a slightly increasing difference between floods is observed with increasing return periods, especially observed in the comparison of the 0.22° against the 0.11° resolution, where the range of values slightly widens with increasing return periods. This is further discussed in Sect. 5.3.

Figure 11 displays the relative biases between the flood indicators for the different return periods divided into two groups. The first group consists of catchments smaller than 1000 km^2 (named s) and the second group consists of

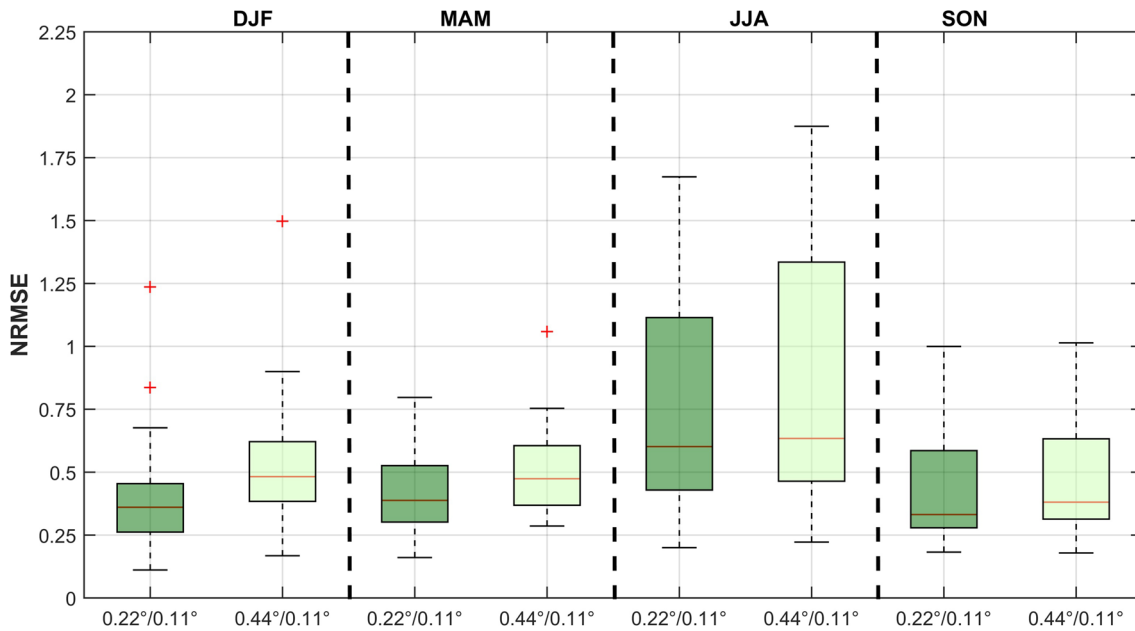


Fig. 9 Seasonal NRMSE values of the comparisons between streamflows generated with RCM outputs at different spatial resolutions. The winter (DJF), spring (MAM), summer (JJA) and fall (SON) sea-

sons are presented from left to right. For each season, the $0.22^\circ/0.11^\circ$ (dark green) and the $0.44^\circ/0.11^\circ$ (light green) comparisons are pre-

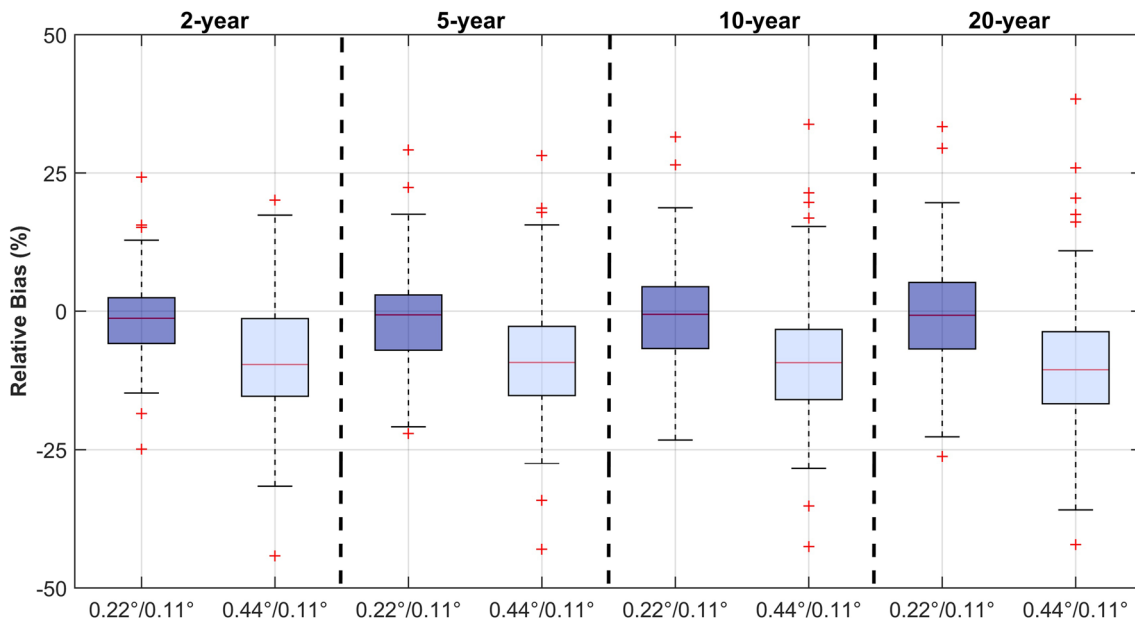


Fig. 10 Relative biases (%) between the summer-fall flood indicators (2-, 5-, 10- and 20-year return periods) from the different CRCM5 resolutions. The 2-year, 5-year, 10-year and 20-year return

periods are presented from left to right. For each return period, the $0.22^\circ/0.11^\circ$ (dark blue) and the $0.44^\circ/0.11^\circ$ (light blue) comparisons are presented

catchments larger than 3000 km^2 (named L). Overall, the group of smaller catchments show larger differences than the group of larger catchments. This is true for both comparisons the $0.22^\circ/0.11^\circ$ and the $0.44^\circ/0.11^\circ$. The observed

differences also show an increase with longer return periods (i.e., from 2-year to 20-year return period), especially in the $0.44^\circ/0.11^\circ$ comparisons.

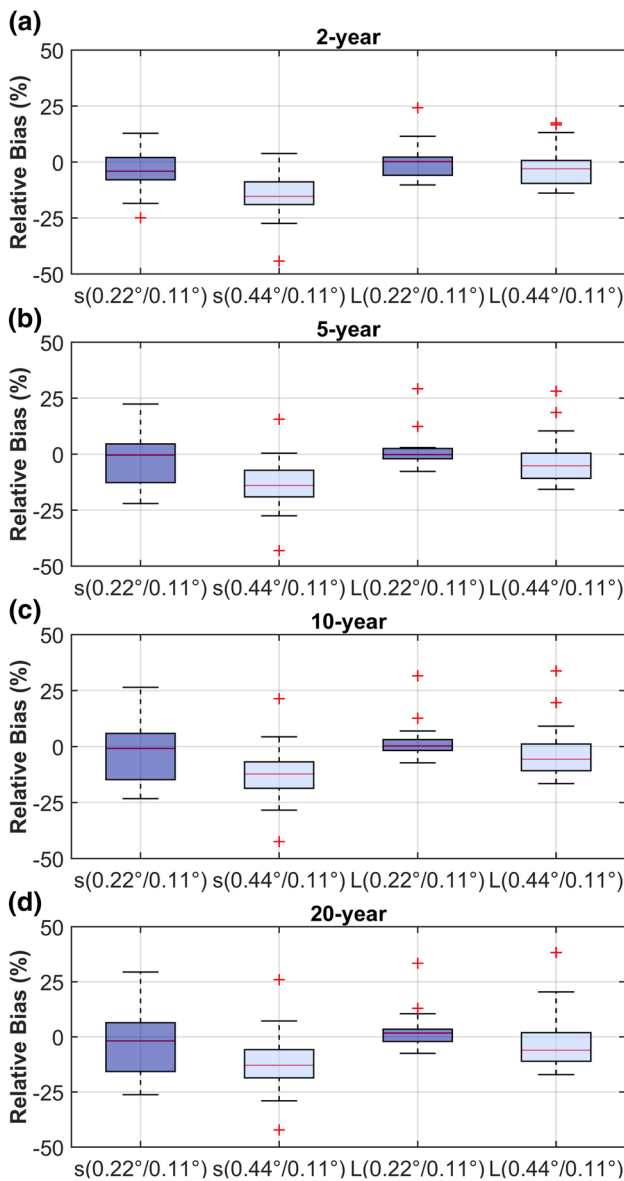


Fig. 11 Relative biases (%) between the summer–fall flood indicators (2-, 5-, 10- and 20-year return periods) from the different CRCM5 resolutions grouped by small (s) and large (L) basins. The first panel **a** presents the comparisons of 2-year return periods, the second panel **b** the comparisons of 5-year return periods, the third panel **c** the comparisons of 10-year return periods and the fourth panel **d** the comparisons of the 20-year return periods. The $0.22^\circ/0.11^\circ$ (dark blue) and the $0.44^\circ/0.11^\circ$ comparisons (light blue) are presented for each indicator

5 Discussion and conclusions

5.1 Effects of RCM spatial resolution on RCM outputs

Seasonal intercomparisons of datasets with different spatial resolutions were performed for temperature and precipitation

outputs. In an attempt to isolate the spatial resolution as the studied variable, all datasets issued from the CRCM5 shared the same configuration, except for their grids of 0.44° , 0.22° and 0.11° resolutions. The CRCM5 temperature comparisons (Fig. 4) present a clear picture of the spatial resolution effects. It is observed that in some regions of the province, the spatial resolution effect resulted in up to a $3\text{ }^\circ\text{C}$ difference. Although not as important as precipitations for flood event simulations, large biases in temperature can influence water balance through the evaporation rate during the summer. It is therefore important to take into account that in otherwise identical CRCM5 simulations, driven by the exact same reanalysis, spatial resolution can have such a large impact on temperature.

The CRCM5 precipitation outputs were also affected by the spatial resolution (see Fig. 5). The seasonal relative biases of precipitation exposed a clear increase in the relative biases when the spatial resolution was increased, especially during the summer months. The 0.22° and 0.44° resolution precipitations presented a consistently dryer bias than the dataset at finer resolution. For the $0.22^\circ/0.11^\circ$ comparisons, relative biases between 10 and 20%, were observed while the $0.44^\circ/0.11^\circ$ comparison presented values reaching up to a 40% difference in the south of the province, meaning that summer precipitation decreased with decreasing spatial resolution. This could possibly be explained by a more intense evaporation/precipitation cycle due to a better resolution of land and lake elements in the 0.11° simulation. This is in line with a recently accepted paper evaluating the influence of horizontal resolution on atmospheric conditions that can lead to freezing rain (St-Pierre et al. 2018). However, no systematic behaviour was observed during the fall, as dry and humid patches varied all over the province. Despite of the methodological differences, the wet bias observed in high resolution CRCM5 simulation is in line with the analyses presented by Whan and Zwiers (2016) and Martynov et al. (2013), where the CRCM5 presented larger amounts of precipitation when compared with another RCM and reanalyses over some North American regions.

Concerning the variance ratio, the effects were different for each climate variable. The CRCM5 temperatures showed decreases from approximately 10–15% with decreasing spatial resolution during the summer and fall seasons (Fig. 6). For the CRCM5-simulated precipitation, the variance ratios were especially affected in the southern part of the province (Fig. 7), where larger ratios are observed. This was particularly observed during the summer months, during which the variability decreases by up to 50% in some regions of the province, from the finer to the larger resolutions. Overall, the variance of precipitation simulations was more sensitive to spatial resolution than the variance of temperature. These effects were observed during the summer season, which was of the most interest in this study. The observed decreases in

precipitation variances could be very important for future trends of flood events as the decreases in variance could suggest a possible decrease in extreme rainfall events during the seasons. Consequently, there could be decreases in the occurrence of summer–fall flood events, which adds uncertainty to studies of hydrological extremes when using different spatial resolutions. This decrease in variability when decreasing resolution could also be explained in part by the RCM spatial resolution improvements in the 0.11° simulations related to land/lake features and orographic effects, but this remains to be validated.

5.2 Streamflow simulations sensitivity to RCM-spatial resolution

In this work, the streamflow simulation analyses present evidence of the impact of the RCM-spatial resolution on the hydrological modelling results. These results were expected, considering the systematic effects observed in the precipitation and temperature simulations that were used to feed the hydrological model. The combination of warmer temperatures observed in Fig. 4 and of the decreases in precipitation amounts presented in Fig. 5 favored the differences between streamflow simulations. These results, concerning the RCM outputs, are in line with a recent study presented by Lucas-Picher et al. (2016), in which an increase in precipitation was found in the finer CRCM5 simulations during the summer months (June, July and August). Curry et al. (2016a, b) also found similar trends when comparing precipitation datasets issued from the fourth version of the CRCM over three river basins, where the finer RCM simulations presented better simulations of precipitation extremes when compared to observations. On the other hand, it is important to recall that the few basins that presented bad performances during the calibration and validation process of the present study can bring additional uncertainties to our results.

5.3 Flood indicators

From Fig. 10, the analysis of flood indicators revealed that the CRCM5 spatial resolution impacted the probability of occurrence of flooding events. The relative biases were shown to gradually increase with longer return periods. In essence, this means that for the 20-year return period (i.e., the lowest probability of occurrence) the difference between summer–fall peak flows was larger than for a 2-year return period, a less-extreme flood. This result agrees with the analyses presented by Lobjigeois et al. (2014), in which finer precipitation simulations were found to significantly impact flood simulations over catchments with highly variable precipitation patterns.

It is also interesting to note that there was a systematic bias present in the $0.44^\circ/0.11^\circ$ comparison in Fig. 10. It can

be seen that the 0.44° simulation has a 10–15% negative bias compared to the 0.11° simulation for all return periods. In contrast, the 0.22° and 0.11° comparison shows that there is some variability, but that the median bias is practically nonexistent. This might mean that for the simulation of summer flood events, resolutions finer than 0.22° do not necessarily provide more usable information. However, it is expected that future RCM development will allow the resolution of more physical processes than is currently possible with available computing resources. This will necessarily entail much finer resolutions, which is expected to improve the simulation quality. It will then be important to distinguish the improvements that are due to spatial resolution from those that are due to the improved process representation.

5.4 Streamflow simulations and catchment size

The RCM spatial resolution impact is likely to be different, depending on the size of the catchment. This has already been pointed out in the literature, where some studies show that streamflow modelling impacts or improvements are related to catchment characteristics such as size and spatial rainfall variability (Lobjigeois et al. 2014; Zhao et al. 2013). Thus, it was expected that small basins would be more sensitive to the increasing spatial resolution, as regional climate patterns are unable to adequately represent detailed trends due to the size of the RCM grid. In other words, fewer grid points fall within a smaller area than within a larger area. For this reason, the analysis presented in Fig. 11 was carried out to explore the sensitivity of flood simulations to the CRCM5 spatial resolution according to catchment size. The figure confirms that the small catchments have larger relative biases due to the climate data's spatial resolution. Moreover, the observed effects systematically increased with longer return periods, meaning that larger impacts were observed in the “most” extreme flood events (i.e., 20-year return period).

5.5 Concluding remarks

This study has explored the uncertainty in flood simulations due to the CRCM5 spatial resolution. It was shown that there is a clear impact between the simulations produced with identical RCMs but different spatial resolution. This study was not meant to inform on the quality of the simulations with respect to the observations, but simply to evaluate the differences between the simulations at different resolutions. It was shown that there is a clear effect of spatial resolution, possibly due to differences in land/lake features and improved topography. Knowing that hydrologists use RCM simulations to estimate risk in future climates, it is imperative that this source of uncertainty be studied and detailed for the development of future RCMs.

While the study's objectives were attained, more work is still needed as improved and finer climate datasets and approaches are constantly produced. The obtained results and the methodological limitations of this work bring out additional research possibilities, such as the evaluation of other RCM climate variables, the addition of convection-permitting simulations, the use of different hydrological models, the evaluation of other flood indicators, and the analysis of finer RCM outputs.

Acknowledgements The author would like to thank the Ouranos Consortium on Regional Climatology and Adaptation for the CRCM5 simulations provided, as well as the Consejo Nacional de Ciencia y Tecnología (CONACYT) and the Ministère de l'Économie, de la Science et de l'Innovation for partial funding of this project.

References

- Alexandru A, Elia RD, Laprise R, Separovic L, Biner S (2009) Sensitivity study of regional climate model simulations to large-scale nudging parameters. *Mon Weather Rev* 137:1666–1686. <https://doi.org/10.1175/2008mwr2620.1>
- Alfieri L, Burek P, Feyen L, Forzieri G (2015) Global warming increases the frequency of river floods in Europe. *Hydrol Earth Syst Sci* 19:2247–2260. <https://doi.org/10.5194/hess-19-2247-2015>
- Arnell NW, Lloyd-Hughes B (2014) The global-scale impacts of climate change on water resources and flooding under new climate and socio-economic scenarios. *Clim Change* 122:127–140. <https://doi.org/10.1007/s10584-013-0948-4>
- Arsenault R, Brissette F (2016) Multi-model averaging for continuous streamflow prediction in ungauged basins. *Hydrol Sci J* 61:2443–2454
- Arsenault R, Poulin A, Côté P, Brissette F (2014) Comparison of stochastic optimization algorithms in hydrological model calibration. *J Hydrol Eng* 19:1374–1384
- Arsenault R, Gatien P, Renaud B, Brissette F, Martel J-L (2015) A comparative analysis of 9 multi-model averaging approaches in hydrological continuous streamflow simulation. *J Hydrol* 529:754–767. <https://doi.org/10.1016/j.jhydrol.2015.09.001>
- Beck HE, Dijk AJMV, Roo AD, Miralles DG, McVicar TR, Schellekens J, Bruijnzeel LA (2016) Global-scale regionalization of hydrologic model parameters. *Water Resour Res* 52:3599–3622. <https://doi.org/10.1002/2015wr018247>
- Beven K (2016) Facets of uncertainty: epistemic uncertainty, non-stationarity, likelihood, hypothesis testing, and communication. *Hydrol Sci J* 61:1652–1665. <https://doi.org/10.1080/0262667.2015.1031761>
- Biner S, Caya D, Laprise R, Spacek L (2000) Nesting of RCMs by imposing large scales. *World Meteorol Organ Publ* 2000:7.3
- Chan SC, Kendon EJ, Fowler HJ, Blenkinsop S, Ferro CAT, Stephenson DB (2013) Does increasing the spatial resolution of a regional climate model improve the simulated daily precipitation? *Clim Dyn* 41:1475–1495. <https://doi.org/10.1007/s00382-012-1568-9>
- Chebana F, Ouarda TBMJ (2011) Multivariate quantiles in hydrological frequency analysis. *Environmetrics* 22:63–78. <https://doi.org/10.1002/env.1027>
- Chen J, Brissette FP, Leconte R (2011) Uncertainty of downscaling method in quantifying the impact of climate change on hydrology. *J Hydrol* 401:190–202
- Côté J, Gravel S, Méthot A, Patoine A, Roch M, Staniforth A (1998) The operational CMC–MRB global environmental multiscale (GEM) model. Part I: design considerations and formulation. *Mon Weather Rev* 126:1373–1395. [https://doi.org/10.1175/1520-0493\(1998\)126%3c1373:tocmge%3e2.0.co;2](https://doi.org/10.1175/1520-0493(1998)126%3c1373:tocmge%3e2.0.co;2)
- Crochemore L et al (2015) Comparing expert judgement and numerical criteria for hydrograph evaluation. *Hydrol Sci J* 60:402–423. <https://doi.org/10.1080/0262667.2014.903331>
- Curry CL, Tencer B, Whan K, Weaver AJ, Giguère M, Wiebe E (2016a) Searching for added value in simulating climate extremes with a high-resolution regional climate model over western Canada. *Atmos Ocean* 54:364–384
- Curry CL, Tencer B, Whan K, Weaver AJ, Giguère M, Wiebe E (2016b) Searching for added value in simulating climate extremes with a high-resolution regional climate model over Western Canada. II: basin-scale results. *Atmos Ocean* 54:385–402
- Dankers R, Feyen L (2008) Climate change impact on flood hazard in Europe: an assessment based on high-resolution climate simulations. *J Geophys Res Atmos* (1984–2012). <https://doi.org/10.1029/2007jd009719>
- Dankers R, Christensen OB, Feyen L, Kalas M, de Roo A (2007) Evaluation of very high-resolution climate model data for simulating flood hazards in the Upper Danube Basin. *J Hydrol* 347:319–331. <https://doi.org/10.1016/j.jhydrol.2007.09.055>
- Dankers R et al (2014) First look at changes in flood hazard in the Inter-Sectoral Impact Model Intercomparison Project ensemble. *Proc Natl Acad Sci* 111:3257–3261. <https://doi.org/10.1073/pnas.1302078110>
- Das J, Umamahesh NV (2018) Assessment of uncertainty in estimating future flood return levels under climate change. *Nat Hazards* 93:109–124. <https://doi.org/10.1007/s11069-018-3291-2>
- Ekström M, Gilletland E (2017) Assessing convection permitting resolutions of WRF for the purpose of water resource impact assessment and vulnerability work: a southeast Australian case study. *Water Resour Res* 53:726–743. <https://doi.org/10.1002/2016WR019545>
- Essou GRC, Brissette F, Lucas-Picher P (2017) Impacts of combining reanalyses and weather station data on the accuracy of discharge modelling. *J Hydrol* 545:120–131. <https://doi.org/10.1016/j.jhydr.2016.12.021>
- Falloon P, Challinor A, Dessai S, Hoang L, Johnson J, Koehler A-K (2014) Ensembles and uncertainty in climate change impacts. *Front Environ Sci* 2:33
- Fortin V, Turcotte R (2006) Le modèle hydrologique MOHYSE Note de cours pour SCA7420. Département des sciences de la terre et de l'atmosphère, Université du Québec à Montréal, Québec
- Giuntoli I, Vidal J, Prudhomme C, Hannah D (2015) Future hydrological extremes: the uncertainty from multiple global climate and global hydrological models. *Earth Syst Dyn* 6:267–285
- Graham LP, Andréasson J, Carlsson B (2007) Assessing climate change impacts on hydrology from an ensemble of regional climate models, model scales and linking methods—a case study on the Lule River basin. *Clim Change* 81:293–307. <https://doi.org/10.1007/s10584-006-9215-2>
- Gupta HV, Kling H, Yilmaz KK, Martinez GF (2009) Decomposition of the mean squared error and NSE performance criteria: implications for improving hydrological modelling. *J Hydrol* 377:80–91
- Hagemann S et al (2013) Climate change impact on available water resources obtained using multiple global climate and hydrology models. *Earth Syst Dyn* 4:129–144
- Hansen N, Ostermeier A (1997) Convergence properties of evolution strategies with the derandomized covariance matrix adaptation: the CMA-ES. *Eufit* 97:650–654

- Hawkins E, Osborne TM, Ho CK, Challinor AJ (2013) Calibration and bias correction of climate projections for crop modelling: an idealised case study over Europe. *Agric For Meteorol* 170:19–31
- Hertwig E, von Storch J-S, Handorf D, Dethloff K, Fast I, Krismer T (2015) Effect of horizontal resolution on ECHAM6-AMIP performance. *Clim Dyn* 45:185–211. <https://doi.org/10.1007/s00382-014-2396-x>
- Huang S et al (2016) Evaluation of an ensemble of regional hydrological models in 12 large-scale river basins worldwide. *Clim Change* 141:381–397. <https://doi.org/10.1007/s10584-016-1841-8>
- Irambona C, Music B, Nadeau DF, Mahdi TF, Strachan IB (2016) Impacts of boreal hydroelectric reservoirs on seasonal climate and precipitation recycling as simulated by the CRCM5: a case study of the La Grande River watershed, Canada. *Theor Appl Climatol* 131:1529–1544. <https://doi.org/10.1007/s00704-016-2010-8>
- Kain JS, Fritsch JM (1990) A one-dimensional entraining/detraining plume model and its application in convective parameterization. *J Atmos Sci* 47:2784–2802. [https://doi.org/10.1175/1520-0469\(1990\)047%3c2784:aodepm%3e2.0.co;2](https://doi.org/10.1175/1520-0469(1990)047%3c2784:aodepm%3e2.0.co;2)
- Kendon EJ et al (2017) Do convection-permitting regional climate models improve projections of future precipitation change? *Bull Am Meteorol Soc* 98:79–93. <https://doi.org/10.1175/bams-d-15-0004.1>
- Klavans JM, Poppick A, Sun S, Moyer EJ (2017) The influence of model resolution on temperature variability. *Clim Dyn* 48:3035–3045. <https://doi.org/10.1007/s00382-016-3249-6>
- Kling H, Fuchs M, Paulin M (2012) Runoff conditions in the upper Danube basin under an ensemble of climate change scenarios. *J Hydrol* 424–425:264–277. <https://doi.org/10.1016/j.jhydrol.2012.01.011>
- Kundzewicz ZW et al (2014) Flood risk and climate change: global and regional perspectives. *Hydrol Sci J* 59:1–28. <https://doi.org/10.1080/02626667.2013.857411>
- Kundzewicz ZW et al (2017) Differences in flood hazard projections in Europe—their causes and consequences for decision making. *Hydrol Sci J* 62:1–14. <https://doi.org/10.1080/02626667.2016.1241398>
- Kundzewicz ZW, Krysanova V, Benestad RE, Hov Ø, Piniewski M, Otto IM (2018) Uncertainty in climate change impacts on water resources. *Environ Sci Policy* 79:1–8. <https://doi.org/10.1016/j.envsci.2017.10.008>
- Kuo H-L (1965) On formation and intensification of tropical cyclones through latent heat release by cumulus convection. *J Atmos Sci* 22:40–63
- Loaiciga HA, Leipnik RB (1999) Analysis of extreme hydrologic events with Gumbel distributions: marginal and additive cases. *Stoch Environ Res Risk Assess* 13:251–259. <https://doi.org/10.1007/s004770050042>
- Lobligois F, Andréassian V, Perrin C, Tabary P, Loumagne C (2014) When does higher spatial resolution rainfall information improve streamflow simulation? An evaluation using 3620 flood events. *Hydrol Earth Syst Sci* 18:575–594. <https://doi.org/10.5194/hess-18-575-2014>
- Lucas-Picher P, Cattiaux J, Bougie A, Laprise R (2015a) How does large-scale nudging in a regional climate model contribute to improving the simulation of weather regimes and seasonal extremes over North America? *Clim Dyn* 46:929–948. <https://doi.org/10.1007/s00382-015-2623-0>
- Lucas-Picher P, Riboult P, Somot S, Laprise R (2015b) Reconstruction of the Spring 2011 Richelieu River flood by two regional climate models and a hydrological model. *J Hydrometeorol* 16:36–54. <https://doi.org/10.1175/jhm-d-14-0116.1>
- Lucas-Picher P, Laprise R, Winger K (2016) Evidence of added value in North American regional climate model hindcast simulations using ever-increasing horizontal resolutions. *Clim Dyn*. <https://doi.org/10.1007/s00382-016-3227-z>
- Mahajan S, Evans KJ, Branstetter M, Anantharaj V, Leifeld JK (2015) Fidelity of precipitation extremes in high resolution global climate simulations. *Proced Comput Sci* 51:2178–2187. <https://doi.org/10.1016/j.procs.2015.05.492>
- Marques FJ, Coelho CA, de Carvalho M (2015) On the distribution of linear combinations of independent Gumbel random variables. *Stat Comput* 25:683–701. <https://doi.org/10.1007/s1122-014-9453-5>
- Martynov A, Laprise R, Sushama L, Winger K, Šeparović L, Dugas B (2013) Reanalysis-driven climate simulation over CORDEX North America domain using the Canadian Regional Climate Model, version 5: model performance evaluation. *Clim Dyn* 41:2973–3005. <https://doi.org/10.1007/s00382-013-1778-9>
- Mearns LO, Bukovsky M, Pryor SC, Magaña V (2018) Downscaling of climate information. In: Lloyd EA, Winsberg E (eds) Climate modelling: philosophical and conceptual issues. Springer, Cham, pp 199–269. https://doi.org/10.1007/978-3-319-65058-6_8
- Mendoza PA et al (2016) Effects of different regional climate model resolution and forcing scales on projected hydrologic changes. *J Hydrol* 541:1003–1019. <https://doi.org/10.1016/j.jhydr.2016.08.010>
- Miguez-Macho G, Stenchikov GL, Robock A (2004) Spectral nudging to eliminate the effects of domain position and geometry in regional climate model simulations. *J Geophys Res Atmos* 109:D13
- Minville M, Brissette F, Leconte R (2008) Uncertainty of the impact of climate change on the hydrology of a nordic watershed. *J Hydrol* 358:70–83
- Naz BS, Kao S-C, Ashfaq M, Rastogi D, Mei R, Bowling LC (2016) Regional hydrologic response to climate change in the conterminous United States using high-resolution hydroclimate simulations. *Glob Planet Change* 143:100–117. <https://doi.org/10.1016/j.gloplacha.2016.06.003>
- Oyerinde G, Houmtondji F, Lawin A, Odofin A, Afouda A, Diekkrüger B (2017) Improving hydro-climatic projections with bias-correction in Sahelian Niger Basin, West Africa. *Climate* 5:8
- Prein AF, Gobiet A, Suklitsch M, Truhetz H, Awan NK, Keuler K, Georgievski G (2013) Added value of convection permitting seasonal simulations. *Clim Dyn* 41:2655–2677. <https://doi.org/10.1007/s00382-013-1744-6>
- Prein AF et al (2015) A review on regional convection-permitting climate modeling: demonstrations, prospects, and challenges. *Rev Geophys* 53:323–361. <https://doi.org/10.1002/2014rg000475>
- Riboult P, Brissette F (2015) Climate change impacts and uncertainties on spring flooding of Lake Champlain and the Richelieu River JAWRA. *J Am Water Resour Assoc* 51:776–793
- Roudier P, Andersson JCM, Donnelly C, Feyen L, Gruell W, Ludwig F (2016) Projections of future floods and hydrological droughts in Europe under a + 2 °C global warming. *Clim Change* 135:341–355. <https://doi.org/10.1007/s10584-015-1570-4>
- Roy P, Gachon P, Laprise R (2014) Sensitivity of seasonal precipitation extremes to model configuration of the Canadian Regional Climate Model over eastern Canada using historical simulations. *Clim Dyn* 43:2431–2453
- Sanchez-Gomez E, Somot S, Déqué M (2009) Ability of an ensemble of regional climate models to reproduce weather regimes over Europe-Atlantic during the period 1961–2000. *Clim Dyn* 33:723–736. <https://doi.org/10.1007/s00382-008-0502-7>
- Sandvik MI, Sorteberg A, Rasmussen R (2018) Sensitivity of historical orographically enhanced extreme precipitation events to idealized temperature perturbations. *Clim Dyn* 50:143–157. <https://doi.org/10.1007/s00382-017-3593-1>
- Separovic L, de Elia R, Laprise R (2012) Impact of spectral nudging and domain size in studies of RCM response to parameter

- modification. *Clim Dyn* 38:1325–1343. <https://doi.org/10.1007/s00382-011-1072-7>
- Separovic L et al (2013) Present climate and climate change over North America as simulated by the fifth-generation Canadian regional climate model. *Clim Dyn* 41:3167–3201. <https://doi.org/10.1007/s00382-013-1737-5>
- Storch HV, Langenberg H, Feser F (2000) A spectral nudging technique for dynamical downscaling purposes. *Mon Weather Rev* 128:3664–3673. [https://doi.org/10.1175/1520-0493\(2000\)128%3c3664:asntfd%3e2.0.co;2](https://doi.org/10.1175/1520-0493(2000)128%3c3664:asntfd%3e2.0.co;2)
- St-Pierre M, Thériault JM, Paquin D (2018) Influence of the model horizontal resolution on atmospheric conditions leading to freezing rain in regional climate simulations. *Atmos Ocean* 2019:1
- Terai CR, Caldwell PM, Klein SA, Tang Q, Branstetter ML (2017) The atmospheric hydrologic cycle in the ACME v0.3 model. *Clim Dyn.* <https://doi.org/10.1007/s00382-017-3803-x>
- Teufel B et al (2017) Investigation of the 2013 Alberta flood from weather and climate perspectives. *Clim Dyn* 48:2881–2899. <https://doi.org/10.1007/s00382-016-3239-8>
- Teutschbein C, Seibert J (2010) Regional climate models for hydrological impact studies at the catchment scale: a review of recent modeling strategies. *Geogr Compass* 4:834–860
- Thirel G et al (2015) Hydrology under change: an evaluation protocol to investigate how hydrological models deal with changing catchments. *Hydrol Sci J* 60:1184–1199. <https://doi.org/10.1080/0262667.2014.967248>
- Trudel M, Doucet-Généreux P-L, Leconte R (2017) Assessing river low-flow uncertainties related to hydrological model calibration and structure under climate change conditions. *Climate* 5:19
- Veijalainen N, Lotsari E, Alho P, Vehviläinen B, Käyhkö J (2010) National scale assessment of climate change impacts on flooding in Finland. *J Hydrol* 391:333–350
- Velázquez J, Anctil F, Perrin C (2010) Performance and reliability of multimodel hydrological ensemble simulations based on seventeen lumped models and a thousand catchments. *Hydrol Earth Syst Sci* 14:2303–2317
- Vetter T et al (2017) Evaluation of sources of uncertainty in projected hydrological changes under climate change in 12 large-scale river basins. *Clim Change* 141:419–433. <https://doi.org/10.1007/s10584-016-1794-y>
- Wasko C, Sharma A (2017) Global assessment of flood and storm extremes with increased temperatures. *Sci Rep* 7:7945. <https://doi.org/10.1038/s41598-017-08481-1>
- Wehner MF, Smith RL, Bala G, Duffy P (2010) The effect of horizontal resolution on simulation of very extreme US precipitation events in a global atmosphere model. *Clim Dyn* 34:241–247. <https://doi.org/10.1007/s00382-009-0656-y>
- Wehner MF et al (2014) The effect of horizontal resolution on simulation quality in the community atmospheric model, CAM5.1. *J Adv Model Earth Syst* 6:980–997. <https://doi.org/10.1002/2013ms000276>
- Wehner M, Arnold J, Knutson T, Kunkel K, LeGrande A (2017) Droughts, floods, and hydrology
- Whan K, Zwiers F (2016) Evaluation of extreme rainfall and temperature over North America in CanRCM4 and CRCM5. *Clim Dyn* 46:3821–3843. <https://doi.org/10.1007/s00382-015-2807-7>
- Wilby RL (2005) Uncertainty in water resource model parameters used for climate change impact assessment. *Hydrol Process* 19:3201–3219
- Wilby RL, Harris I (2006) A framework for assessing uncertainties in climate change impacts: low-flow scenarios for the River Thames, UK. *Water Resour Res* 42:2
- Yue S, Ouarda TBMJ, Bobée B, Legendre P, Bruneau P (1999) The Gumbel mixed model for flood frequency analysis. *J Hydrol* 226:88–100. [https://doi.org/10.1016/S0022-1694\(99\)00168-7](https://doi.org/10.1016/S0022-1694(99)00168-7)
- Zeng X-M, Wang M, Zhang Y, Wang Y, Zheng Y (2016) Assessing the effects of spatial resolution on regional climate model simulated summer temperature and precipitation in China: a case study. *Adv Meteorol* 2016:12. <https://doi.org/10.1155/2016/7639567>
- Zhao F, Zhang L, Chiew FHS, Vaze J, Cheng L (2013) The effect of spatial rainfall variability on water balance modelling for south-eastern Australian catchments. *J Hydrol* 493:16–29. <https://doi.org/10.1016/j.jhydrol.2013.04.028>

Publisher's Note Springer Nature remains neutral with regard to jurisdictional claims in published maps and institutional affiliations.